Control of a hydraulic servo system using sliding mode with an integral and realizable reference compensation

Emna Kolsi-Gdoura * **Moez Feki** ** **Nabil Derbel** *

* *Control and Energy Management Laboratory (CEMLab), National Engineering School of Sfax, Tunisia. (e-mail: kolsiemna@yahoo.fr, n.derbel@enis.rnu.tn).*
** *École Supérieure des Sciences et de Technologie de Hammam Sousse, University of Sousse, Tunisia. (e-mail: moez.feki@enig.rnu.tn)*

Abstract: In this paper a control law was designed to accurately control the rod position of hydraulic servo system. In fact, due to its having a nonlinear model, the hydraulic servo system is not accurately stabilized by a proportional controller and suffers from wind up phenomenon when applying the PI controller. To overcome the problems encountered by the action of these linear controllers, a sliding mode controller with an integral and realizable reference compensation is used to obtain an accurate position in addition to having a short settling time. The efficiency of the proposed scheme is illustrated using numerical simulations.

Keywords: Hydraulic servo system; sliding mode control; actuator saturation; realizable reference.

1. INTRODUCTION

Hydraulic systems have been used in industry in a wide number of applications where large inertia and torque loads have to be handled, providing a high degree of both accuracy and performance (Merritt, 1967). The hydraulic servo system, among others, is perhaps the most important system for position servo applications because it takes the advantages of both the large output power of traditional hydraulic systems and the rapid response of electric systems (Merritt, 1967; Viersma, 1980). Typical applications of hydraulic position servo systems include lifting payloads, shaping hard material (*e.g.* shaping iron sheets); other applications consists in accurate metal-working. Although some of these applications are handled in open loop control, which does not require much studies, several other applications are to be handled in closed loop control which makes the control task more difficult due to the need for accurate servovalve model.

Due to the highly nonlinear property of hydraulic servo systems, the controller design based on local linearization is a commonly used approach (Merritt, 1967; Viersma, 1980). However such approach yields to conservative controllers that sacrifice performance and robustness in favor of simplicity.

To achieve higher performances, nonlinear control methods and intelligent methods have been used to control hydraulic servo systems. In (Feki et al., 1999), the input/output linearizing controller has been used to track a predetermined force profile. Although, the intended results were attained, the robustness to parameter variations was not guaranteed. To account for presence of unmodeled dynamics, parametric uncertainties and external disturbances, adaptive controllers have been proposed in (Yao et al., 2001; Ahn and Dinh, 2009) where the parameter uncertainties occur linearly. To handle the case where unknown parameters occur nonlinearly such as the cylinder volume, a controller using the adaptive control theory and the backstepping technique has been designed in (Sirouspour and Salcudean, 2000; Guan and Pan, 2008; Ursu et al., 2013).

In (Truong and Ahn, 2009), authors suggested a grey prediction model combined with a fuzzy PID controller to achieve a predetermined force and to improve the control quality of the loading system while eliminating or reducing the disturbance. PID controllers have also been enhanced using fuzzy methods (Mihajlov et al., 2002; Has et al., 2013), genetic algorithm (Aly, 2011) and feed forward compensation by pole-zero placement (Jian-jun et al., 2012) to obtain accurate position control.

Variable structure control (VSC) is an other controller that has been widely used to cope with systems with parameter uncertainties and unknown nonlinear dynamics (Khebbache and Tadjine, 2013; Rossomando et al., 2014; Kolsi-Gdoura et al., 2013). In (Hwang and Lan, 1994), a time-varying switching gain, a second-order relation between sliding surface and uncertainties and a boundary layer for the sliding surface, is employed to deal with the position control. In (Miao et al., 2008), a novel control scheme for hydraulic servo systems with large frictional torques is proposed based on a sliding-mode variable structure controller combined with a frictional state observer. In (Chen et al., 2005) position control has been addressed using VSC with varying boundary layers in order to improve the tracking performance by reducing the boundary width and decreasing the chattering effect by increasing the boundary width. To achieve accurate position control in the presence of important friction nonlinearities, the sliding mode control has also been used in (Tafazoli et al., 1998; Bonchis et al., 2001). In (Indrawanto, 2011), a single rigid hydraulically actuated manipulator was controlled using the sliding mode controller to count for the changing of inertia moment of the manipulator as well as the effect of fiction.

The present paper deals with the design of a simple controller that may achieve the reference position in presence of parameter uncertainty and perturbation in addition to actuator saturation. This issue has been dealt with in (Kolsi-Gdoura et al., 2013) for a hydraulic servo system with a symmetric piston that can be modeled with a three dimensional system where the states are the differential pressure, the velocity and the position of the rod. However, in this paper, we deal with the more general case that is a hydraulic servo system with a non symmetric piston. Thus the system has to be modeled with a fourth order nonlinear dynamical system where in addition to the position and the velocity of the rod, the pressures in each chamber of the cylinder represent a new state variable. Besides, we add in this paper an observer design to estimate the unmeasurable states, thus achieving an output control strategy. The observer design is based on the sliding mode theory.

To accomplish the prescribed aim, the effects of a proportional (P) and a proportional integral (PI) control is presented in the second section. In section three, an enhanced sliding mode controller by using an integral surface and realizable reference is designed to shorten the reaching mode and thus to obtain a short settling time. Numerical simulation results are presented to illustrate the efficiency of the proposed control method. The fourth section, is devoted to the sliding observer design and the use of the estimated states to design the controller and achieve the output feedback design. Finally, the conclusion is drawn in the last section.

2. PROBLEM STATEMENT

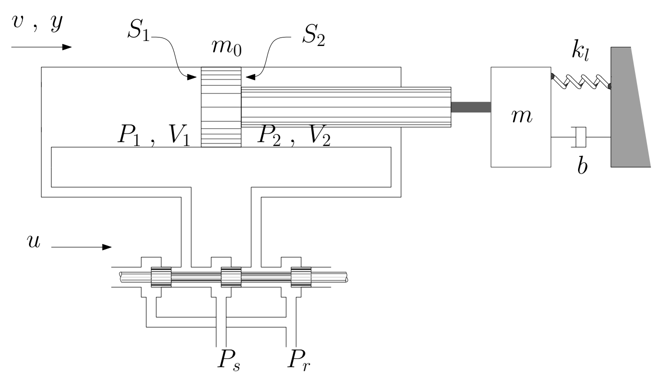

Fig. 1. Hydraulic servo system

The hydraulic servo system depicted in figure 1 is modeled by the following dynamical system Feki and Richard (2005); Feki et al. (1999)

$$\dot{P}_1 = \frac{B}{V_0 + S_1 y}\Big(Q_1 - S_1 v\Big) \; , \tag{1a}$$

$$\dot{P}_2 = \frac{B}{V_0 - S_2 y}\Big(Q_2 + S_2 v\Big) \; , \tag{1b}$$

$$\dot{v} = \frac{1}{m + m_0}(S_1 P_1 - S_2 P_2 - bv - k_l y) \; , \tag{1c}$$

$$\dot{y} = v + d \; , \tag{1d}$$

where the flow rates Q_1 and Q_2 are:

$$Q_1 = \begin{cases} ku\sqrt{P_s - P_1} + \dfrac{\alpha(P_s + P_r - 2P_1)}{1 + \gamma u} & \text{if } u \geq 0 \\ ku\sqrt{P_1 - P_r} + \dfrac{\alpha(P_s + P_r - 2P_1)}{1 - \gamma u} & \text{if } u < 0 \end{cases} \tag{2}$$

$$Q_2 = \begin{cases} -ku\sqrt{P_2 - P_r} + \dfrac{\alpha(P_s + P_r - 2P_2)}{1 + \gamma u} & \text{if } u \geq 0 \\ -ku\sqrt{P_s - P_2} + \dfrac{\alpha(P_s + P_r - 2P_2)}{1 - \gamma u}, & \text{if } u < 0 \end{cases} \tag{3}$$

with k, α and γ are constants intrinsic to the servovalve and model the flow and the leakage through it.

P_1 and P_2 respectively denote the pressure inside the first and the second chamber of the cylinder, v and y respectively denote the velocity and the position of the rod and $d(t) < d_{max}$ is a bounded constant external perturbation. m_0 is the mass of the rod and m is the mass of the load, V_1 and V_2 are respectively the volume of the first and the second chamber of the cylinder, S_1 and S_2 are respectively the section surface of the first and the second sides of the piston, P_s is the supply pressure(pressure of the pump) and P_r is the return pressure (atmospheric pressure). k_l is the spring stiffness constant and b is the friction coefficient. B is the effective bulk modulus of the fluid and u is the control signal.

Clearly, we notice that the system is highly non linear with respect to the state vector and is also non affine with respect to the control signal u. Thus designing a control law is not a simple task. In addition we consider that the system is under the effect of several mismatched perturbations. Particularly, the spring constant is known with an uncertainty of up to 20% of its nominal value and the jack velocity undergoes an unknown bounded constant perturbation $d < d_{\max}$. Finally, due to practical limitation, the input signal $u(t)$ which is merely the current injected to the servovalve is restrained to maximum allowed values $|u(t)| \leq u_{\max}$.

Nevertheless, one can always start by checking the effect of the proportional and PI controllers which do not require model knowledge. The control signal of a proportional controller is given by $u_p = k_0(y_{ref} - y)$ whereas the PI control signal is given by $u_{pi} = k_0(y_{ref} - y) + k_i \int_0^t (y_{ref} - y)dt$, where y_{ref} is the reference position to be attained. Additionally, the actuator constraint is described by the saturation function:

$$u_{sat} = \frac{1}{2}(|u + u_{\max}| - |u - u_{\max}|) \tag{4}$$

Simulating the system using the parameter values shown in the nomenclature, we obtained the results on figure 2 for the proportional controller and figure 3 for the PI controller. We notice that the proportional controller yields to steady state error (SSE) of 9.1% and a 5% settling time of $T_{s5\%}$ =0.6s. On the other hand, the PI controller eliminates the SSE, but the settling time becomes too long due to wind-up phenomenon, indeed the settling time becomes 2.64s. Using an anti wind-up procedure the settling time is reduced to $T_{s5\%}$ =0.75s as shown in 4.

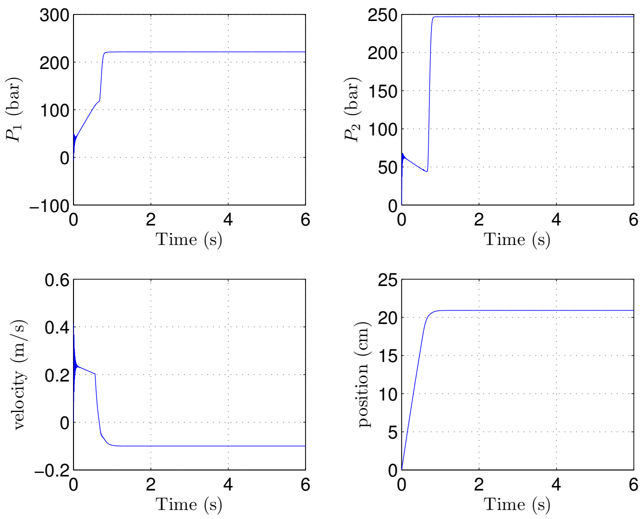

Fig. 2. Position control of the hydraulic servo system under the proportional controller: SSE=9.1% , $T_{s5\%}$ =0.6s.

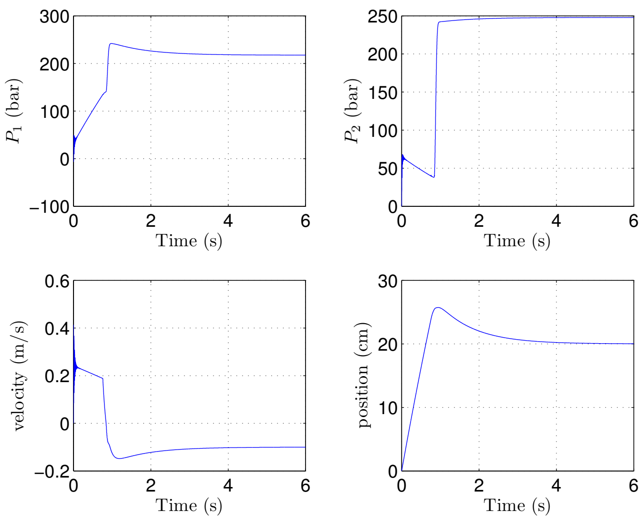

Fig. 3. Position control of the hydraulic servo system under the PI controller: SSE=0 , $T_{s5\%}$ =2.64s.

3. SLIDING MODE CONTROLLER DESIGN

The objective of this section is to design a simple controller while obtaining accurate and fast position control. To attain our aim, we propose a sliding mode controller with an integral surface having the following expression:

$$u = -u_{\max}\mathrm{sign}(\sigma) \quad (5)$$

where σ is the sliding surface defined by:

$$\sigma = C_4\tilde{y}_{int} + C_3\tilde{y} + C_2\tilde{v} + C_1\tilde{P}_2 + \tilde{P}_1 \quad (6)$$

with $\tilde{P}_1 = P_1 - P_{1e}$, $\tilde{P}_2 = P_2 - P_{2e}$, $\tilde{v} = v - v_e$, $\tilde{y} = y - y_{ref}$ and $\tilde{y}_{int} = \int_0^t \tilde{y}dt$. $(P_{1e}, P_{2e}, v_e, y_{ref})$ is the

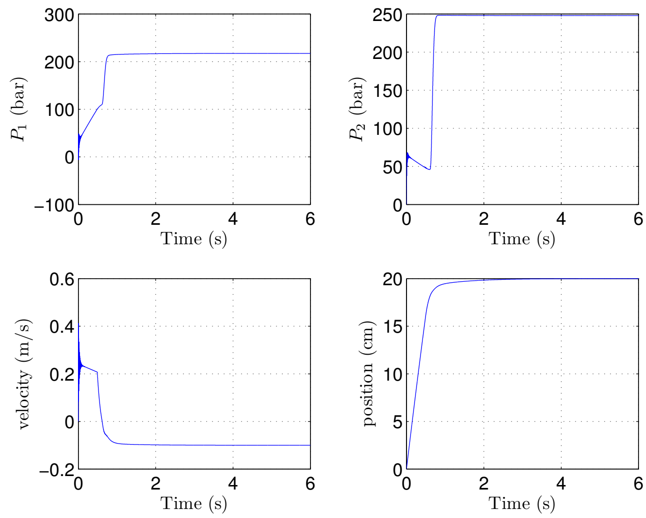

Fig. 4. Position control of the hydraulic servo system under the PI controller with anti wind-up: SSE=0 , $T_{s5\%}$ =0.75s.

unperturbed system equilibrium point when the reference position y_{ref} is attained, and C_4, C_3, C_2 and C_1 are design constants that will be chosen to ensure an asymptotic stability of the system when it is behaving in sliding mode, that is when $\sigma = 0$.

To confine the system behavior to the sliding surface we need to satisfy the attractivity condition $\sigma\dot{\sigma} < 0$. Knowing that when $\sigma < 0$ then $u > 0$ and thus we have:

$$\begin{aligned}\sigma\dot{\sigma} &= C_4\sigma(y - y_{ref}) + C_3\sigma(v + d)\\ &+ C_2\frac{\sigma\Big(S_1P_1 - S_2P_2 - bv - k_l y\Big)}{m + m_0}\\ &+ C_1\frac{B\Big(-ku_{\max}|\sigma|\sqrt{P_2 - P_r} + \frac{\alpha(P_s+P_r-2P_2)}{1+\gamma u_{\max}} + S_2\sigma v\Big)}{V_0 - S_2 y}\\ &+ \frac{B\Big(ku_{\max}|\sigma|\sqrt{P_s - P_1} + \frac{\alpha(P_s+P_r-2P_1)}{1+\gamma u_{\max}} - S_1\sigma v\Big)}{V_0 + S_1 y}\end{aligned}$$

and when $\sigma > 0$ then $u < 0$ thus we have:

$$\begin{aligned}\sigma\dot{\sigma} &= C_4\sigma(y - y_{ref}) + C_3\sigma(v + d)\\ &+ C_2\frac{\sigma\Big(S_1P_1 - S_2P_2 - bv - k_l y\Big)}{m + m_0}\\ &+ C_1\frac{B\Big(-ku_{\max}|\sigma|\sqrt{P_s - P_2} + \frac{\alpha(P_s+P_r-2P_2)}{1+\gamma u_{\max}} + S_2\sigma v\Big)}{V_0 - S_2 y}\\ &+ \frac{B\Big(ku_{\max}|\sigma|\sqrt{P_1 - P_r} + \frac{\alpha(P_s+P_r-2P_1)}{1+\gamma u_{\max}} - S_1\sigma v\Big)}{V_0 + S_1 y}\end{aligned}$$

Thus, to fulfill the attractivity condition, we may choose C_4, C_3, C_2 and C_1 such that:

$$\frac{|C_4(y-y_{ref})+C_3(v+d_{\max})|}{\frac{C_1Bk}{V_0-S_2y}\sqrt{P_2-P_r}-\frac{Bk}{V_0+S_1y}\sqrt{P_s-P_1}} + \frac{\left|\frac{C_2}{m+m_0}(S_1P_1-S_2P_2-bv-k_ly)\right|}{\frac{C_1Bk}{V_0-S_2y}\sqrt{P_2-P_r}-\frac{Bk}{V_0+S_1y}\sqrt{P_s-P_1}} + \frac{\left|\frac{C_1B}{V_0-S_2y}\Big(\alpha(P_s+P_r-2P_2)+S_2v\Big)\right|}{\frac{C_1Bk}{V_0-S_2y}\sqrt{P_2-P_r}-\frac{Bk}{V_0+S_1y}\sqrt{P_s-P_1}} + \frac{\left|\frac{B}{V_0+S_1y}\Big(\alpha(P_s+P_r-2P_2)-S_1v\Big)\right|}{\frac{C_1Bk}{V_0-S_2y}\sqrt{P_2-P_r}-\frac{Bk}{V_0+S_1y}\sqrt{P_s-P_1}} \le u_{\max} \quad \text{if } \sigma<0$$

$$\frac{|C_4(y-y_{ref})+C_3(v+d_{\max})|}{\frac{C_1Bk}{V_0-S_2y}\sqrt{P_s-P_2}-\frac{Bk}{V_0+S_1y}\sqrt{P_1-P_r}} \frac{\left|+\frac{C_2}{m+m_0}(S_1P_1-S_2P_2-bv-k_ly)\right|}{\frac{C_1Bk}{V_0-S_2y}\sqrt{P_s-P_2}-\frac{Bk}{V_0+S_1y}\sqrt{P_1-P_r}} + \frac{\left|\frac{C_1B}{V_0-S_2y}\Big(\alpha(P_s+P_r-2P_2)+S_2v\Big)\right|}{\frac{C_1Bk}{V_0-S_2y}\sqrt{P_s-P_2}-\frac{Bk}{V_0+S_1y}\sqrt{P_1-P_r}} + \frac{\left|\frac{B}{V_0+S_1y}\Big(\alpha(P_s+P_r-2P_2)-S_1v\Big)\right|}{\frac{C_1Bk}{V_0-S_2y}\sqrt{P_s-P_2}-\frac{Bk}{V_0+S_1y}\sqrt{P_1-P_r}} \le u_{\max} \quad \text{if } \sigma>0$$

Obviously, there are infinite choices of C_4, C_3, C_2 and C_1 such that the attainability condition is satisfied. However, there is an additional and necessary condition that should also be satisfied which is the asymptotic stability of the system in sliding mode; that is when the system is confined to $\sigma = 0$. In this case, we have:

$$\tilde{P}_1 = -C_1\tilde{P}_2 - C_2\tilde{v} - C_3\tilde{y} - C_4\tilde{y}_{int} \tag{7}$$

thus the system dynamics may be described as follows:

$$\dot{\tilde{y}}_{int} = \tilde{y}\ , \tag{8a}$$
$$\dot{\tilde{y}} = \tilde{v} + d\ , \tag{8b}$$
$$\dot{\tilde{v}} = \frac{1}{m+m_0}\Big(S_1(-C_1\tilde{P}_2 - C_2\tilde{v} - C_3\tilde{y} - C_4\tilde{y}_{int} + P_{1e}) -S_2(\tilde{P}_2+P_{2e}) - b(\tilde{v}+v_e) - k_l(\tilde{y}+y_{ref})\Big)\ , \tag{8c}$$
$$\dot{\tilde{P}}_2 = \frac{B}{V_0 - S_2(\tilde{y}+y_{ref})}\Big(Q_2 + S_2(\tilde{v}+v_e)\Big)\ , \tag{8d}$$

Since at equilibrium we have $S_1P_{1e} - S_2P_{2e} - bv_e - k_ly_{ref} = 0$ and should we choose

$$C_1 = -\frac{S_2}{S_1} \tag{9}$$

then we get:

$$\dot{\tilde{y}}_{int} = \tilde{y}\ , \tag{10a}$$
$$\dot{\tilde{y}} = \tilde{v} + d\ , \tag{10b}$$
$$\dot{\tilde{v}} = \frac{-S_1C_4\tilde{y}_{int} - (S_1C_3+k_l)\tilde{y} - (S_1C_2+b)\tilde{v}}{m+m_0} \tag{10c}$$
$$\dot{\tilde{P}}_2 = \frac{B}{V_0 - S_2(\tilde{y}+y_{ref})}\Big(Q_2 + S_2(\tilde{v}+v_e)\Big)\ , \tag{10d}$$

Clearly, after application of a control signal $u(x_1, x_2)$, the obtained system (10) is an autonomous system in the triangular form:

$$\dot{x}_1 = f_1(x_1)\ , \tag{11a}$$
$$\dot{x}_2 = f_2(x_1 + x_{1e}, x_2 + x_{2e})\ , \tag{11b}$$

with $x_1 = (\tilde{y}_{int}, \tilde{y}, \tilde{v})$ and $x_2 = \tilde{P}_2$. Using Proposition 1 we may prove the stability of system (10) which is actually confined to behave on the sliding surface.

Proposition 1. Consider the dynamic system defined by (11). Assume that $x_1 = 0$ is an exponentially stable equilibrium for (11-a) and $\dot{x}_2 = f_2(x_{1e}, x_2 + x_{2e})$ is an exponentially bounded system. Moreover, assume that $f_2(x_1 + x_{1e}, x_2 + x_{2e})$ is Lipschitz w.r.t. x_1 and x_2 with constants γ_1 and γ_2 respectively. Then if $\|x_{1e}\| \le \gamma_3$, then $\lim_{t\to\infty} x_1(t) = 0$ and $\|x_2\| < \infty$.

Proof: See the appendix.

Now, to apply the above result to the controlled servo system (10) and to prove that is stable and would reach its reference value, we can easily note that the first three equations form a linear subsystem whose characteristic equation is given by:

$$s^3 + \frac{S_1C_2+b}{m+m_0}s^2 + \frac{S_1C_3+k_l}{m+m_0}s + \frac{S_1C_4}{m+m_0} = 0 \tag{12}$$

Using the pole placement method and imposing a stable multiple pole at $s = -\lambda$ ($\lambda > 0$), one can derive the following conditions for the determination of the control parameters:

$$C_2 = \frac{3\lambda(m+m_0) - b}{S_1} \tag{13}$$
$$C_3 = \frac{3\lambda^2(m+m_0) - k_l}{S_1} \tag{14}$$
$$C_4 = -\frac{\lambda^3(m+m_0)}{S_1} \tag{15}$$

When it comes to the fourth equation which forms the second subsystem, we notice that it is not globally Lipschitz since it includes the square root term. Nevertheless, since the system variables are not supposed to behave in the vicinity of their physical limits, then a local Lipschitz condition is satisfied. It remains now to prove that the second subsystem described by (16) is exponentially bounded.

$$\dot{\tilde{P}}_2 = \begin{cases} \frac{B}{V_0 - S_2y_{ref}}\Big(-ku_{\max}\sqrt{\tilde{P}_2 + P_{2e} - P_r} + \frac{\alpha}{1+\gamma u_{\max}}(P_s + P_r - 2\tilde{P}_2) + S_2v_e\Big) & \text{if } \sigma \le 0 \\ \frac{B}{V_0 - S_2y_{ref}}\Big(ku_{\max}\sqrt{P_s - \tilde{P}_2 - P_{2e}} + \frac{\alpha}{1+\gamma u_{\max}}(P_s + P_r - 2\tilde{P}_2) + S_2v_e\Big) & \text{if } \sigma > 0 \end{cases} \tag{16}$$

Clearly, the subsystem (16) is a switched system where each of which has its own equilibrium point. To prove the exponential boundedness, we use a graphical analysis as shown on Fig. 5.

In blue color, we present $\dot{\tilde{P}}_2$ versus $\tilde{P}_2$ when $\sigma \le 0$ where the solid part represent the effective part of the vector field and the dashed part is not effective since the pressure in the system cannot drop beyond the return pressure. The arrows on the $\tilde{P}_2$ axis point to the left if $\dot{\tilde{P}}_2 < 0$ that is the pressure is decreasing and they point to the right if $\dot{\tilde{P}}_2 > 0$ that is the pressure is increasing. Using similar argument for the case of $\sigma > 0$ shown in black

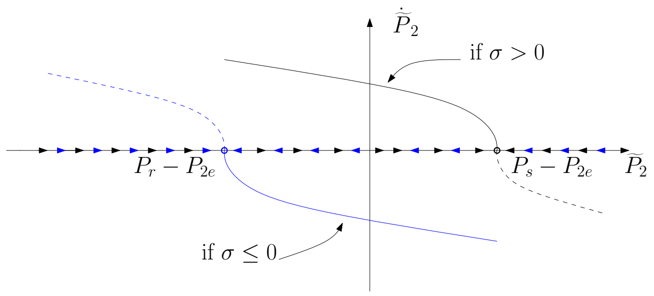

Fig. 5. Graphical analysis to prove the exponential boundedness of $\widetilde{P}_2$.

curve and arrows, we may easily deduce that when the pressure is initiated in the interval $P_2(0) \in (P_r, P_s)$ then $P_2(t)$ remains in that interval for all subsequent time which proves the boundedness of the second subsystem.

Finally using Proposition 1, we may deduce that the reference position is achieved by the servo system under the action of a sliding control signal with an integral surface. Figure 6 delineates the behavior of the so controlled system states in presence of the constant perturbation $d = 0.1$ and an uncertainty in the spring constant of order of 20% and with closed loop poles placed at $\lambda = 15$. We notice that the reference position has been achieved with a settling time $T_{s5\%} = 0.91s$ and an overshoot of about 25%. The rod velocity has been stabilized at $v = -0.1$ to compensate the perturbation d and hence the physical velocity of the system is zero that is the rod is at rest. We also notice that the pressures in the chambers of the piston evolved within the interval (P_r, P_s). Finally, the control signal used to assess the hydraulic servo system is shown in Fig. 7.

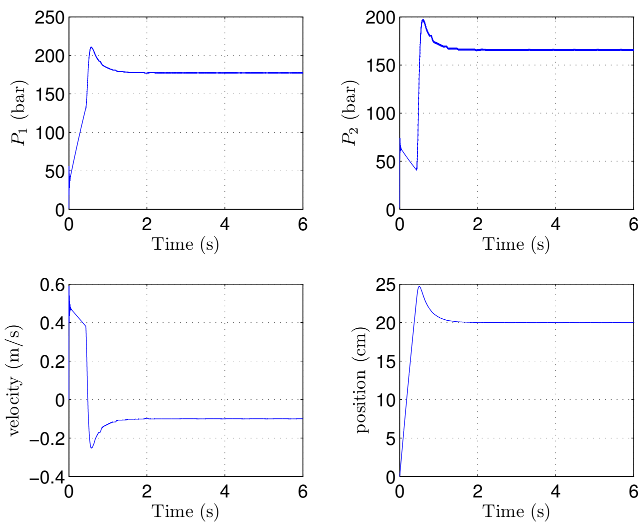

Fig. 6. Position control of the hydraulic servo system under the integral surface sliding mode controller: $\lambda = 15$

To improve the system behavior such as decreasing the settling time and eliminating the overshoot of the system, we may think of decreasing the reaching time needed for the system to attain sliding mode. To do so, we consider the realizable reference that can be attained by the control at each instant, and use that information so that the system behaves as if it is in sliding mode at each instant of the transient time.

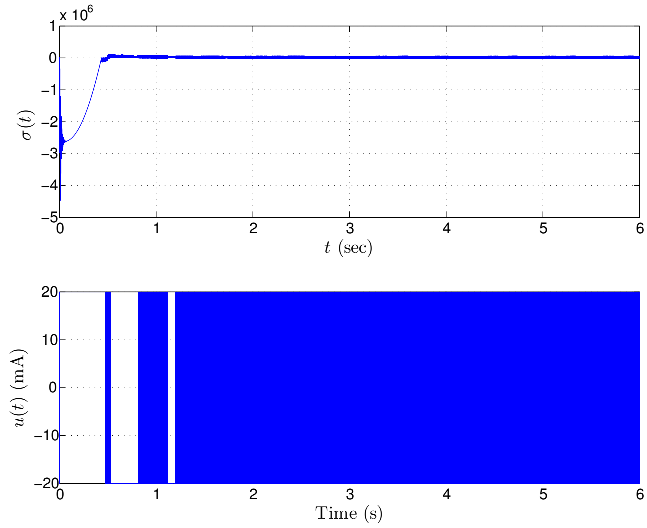

Fig. 7. Sliding surface $\sigma(t)$ and the control signal $u(t)$ used to assess the hydraulic servo system.

Let the realizable reference be denoted by r_{ref}. With the realizable reference, the sliding mode is supposed to be attained that is $\sigma = 0$, then substituting in (6) we get:

$$0 = C_4 \tilde{y}_{int} + C_3(y - r_{ref}) + C_2\tilde{v} + C_1\tilde{P}_2 + \tilde{P}_1 \tag{17}$$

Subtracting (17) from (6), we get:

$$r_{ref} = y_{ref} + \frac{1}{C_3}\sigma \tag{18}$$

Next, we substitute the reference by the realizable reference in the dynamics of the integral state to get:

$$\dot{y}_{int} = y - y_{ref} - \frac{1}{C_3}\sigma = \tilde{y} - \frac{1}{C_3}\sigma \tag{19}$$

Eventually, we get:

$$\dot{\sigma} = \begin{cases} -\frac{C_4}{C_3}\sigma + C_4(y - y_{ref}) + C_3(v + d) \\ +\frac{C_2}{m + m_0}\Big(S_1P_1 - S_2P - bv - k_l y\Big) \\ +\frac{C_1 B}{V_0 - S_2 y}\Big(- k u_{\max}\mathrm{sign}(\sigma)\sqrt{P_2 - P_r} \\ +\frac{\alpha}{1 + \gamma u_{\max}}(P_s + P_r - 2P_2) + S_2 v\Big) \\ +\frac{B}{V_0 + S_1 y}\Big(k u_{\max}\mathrm{sign}(\sigma)\sqrt{P_s - P_1} \\ +\frac{\alpha}{1 + \gamma u_{\max}}(P_s + P_r - 2P_1) - S_1 v\Big) & \text{if } \sigma \leq 0 \\ -\frac{C_4}{C_3}\sigma + C_4(y - y_{ref}) + C_3(v + d) \\ +\frac{C_2}{m + m_0}\Big(S_1P_1 - S_2P_2 - bv - k_l y\Big) \\ +\frac{C_1 B}{V_0 - S_2 y}\Big(- k u_{\max}\mathrm{sign}(\sigma)\sqrt{P_s - P_2} \\ +\frac{\alpha}{1 + \gamma u_{\max}}(P_s + P_r - 2P_2) + S_2 v\Big) \\ +\frac{B}{V_0 + S_1 y}\Big(k u_{\max}\mathrm{sign}(\sigma)\sqrt{P_1 - P_r} \\ +\frac{\alpha}{1 + \gamma u_{\max}}(P_s + P_r - 2P_1) - S_1 v\Big) & \text{if } \sigma > 0 \end{cases}$$

We notice that $\dot{\sigma}$ is now expressed in terms of σ in addition to the expression obtained earlier. This makes the attractivity of the sliding surface σ conditioned by the following relation:

$$\frac{C_4}{C_3} > 0 \tag{20}$$

knowing that $C_4 > 0$, then we need to choose λ such that C_3 is also positive, that is:

$$\lambda > \sqrt{\frac{k_l}{3(m + m_0)}} \tag{21}$$

Figure 8 depicts the behavior of the system states when controlled by the integral sliding controller with the integral state being modified as shown in (19). The closed loop poles are placed at $\lambda = 90$ to satisfy the stability condition (21). We notice that the reference position has been achieved with a settling time $T_{s5\%} = 0.35s$ and an overshoot of about 1.5%. The rod velocity has been again stabilized at $v = -0.1$ to compensate the perturbation d. We also notice that the pressures in the chambers of the piston evolved within the interval (P_r, P_s). Finally, the control signal used to assess the hydraulic servo system is shown in Fig. 9. Clearly, this controller outperforms the previous designed controllers.

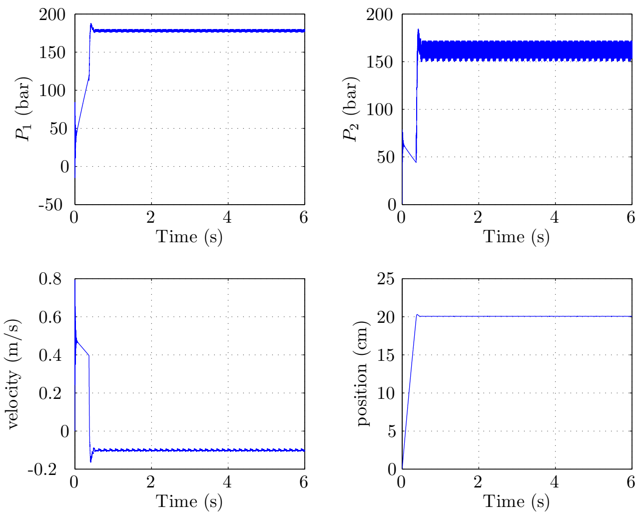

Fig. 8. Position control of the hydraulic servo system under the integral surface sliding mode controller: $\lambda = 90$

We should mention here that we did not deal with the chattering phenomenon since our aim was to construct a simple controller expression. Nevertheless, one way to reduce the chattering phenomenon is to smooth the sign function by choosing for instance the differentiable $\tanh(A\sigma)$ function where A is a gain. We notice that when A is very large then $\tanh(A\sigma) \simeq \text{sign}(\sigma)$. Figure 10 depicts the behavior of the system states when the controller uses a smooth function. We notice the decrease in the chattering phenomenon especially in the pressure and velocity behaviors. Figure 11 depicts the behavior of the controller and the sliding surface when the controller uses a smooth function. Clearly, we notice that the chattering was removed and the average controller signal is applied. To avoid the chattering phenomenon, we have eventually used a smooth saturation function that achieved a chattering free response.

4. SLIDING MODE OBSERVER DESIGN

As we can notice, the controller conceived in the foregoing section implicitly uses all four state variables through the

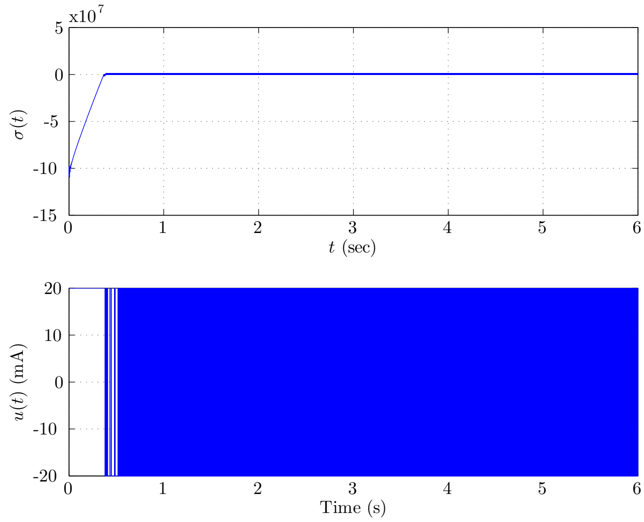

Fig. 9. Sliding surface $\sigma(t)$ and the control signal $u(t)$ used to assess the hydraulic servo system.

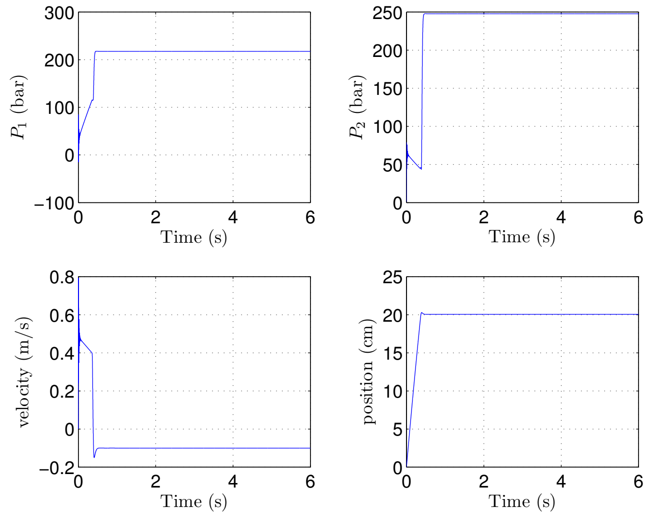

Fig. 10. State behavior of the hydraulic servo system under the integral surface sliding mode controller with smooth saturation function.

sliding surface definition. However, measuring the pressures P_1 and P_2 is a costly task and requires high technology procedure to avoid additional leakage. To circumvent this problem, we propose in this section to design a sliding mode observer that may estimate the required states that are then used to construct the sliding surface.

Before tackling the observer design, it is worth noting that when the rod position y is the measured output, then we may easily check that the hydraulic servo system described by its model (1) is not fully observable. Indeed, the pressures P_1 and P_2 are not observable, however, the difference $S_1P_1 - S_2P_2$ is itself observable if it is defined as a single state. Should we refer to the choice of $C_1 = -\frac{S_2}{S_1}$ given in (9), and to the expression of the sliding surface (6), then we deduce that we only need to estimate the expression $E = S_1P_1 - S_2P_2$ to be able to construct the sliding surface. Therefore, our choice to use a sliding observer is motivated by its robustness and the possibility to achieve the estimation of that expression without the

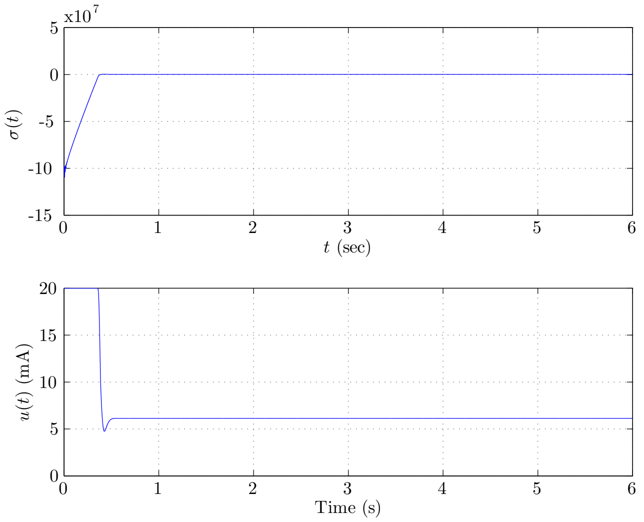

Fig. 11. Sliding surface $\sigma(t)$ and the control signal $u(t)$ used to assess the hydraulic servo system with smooth saturation function.

need to obtain the full model. We here consider the reduced order model of the hydraulic servo system:

$$\dot{E} = f(P_1, P_2, v, y) \tag{22}$$

$$\dot{v} = \frac{1}{m+m_0}(E - bv - (k_l + \delta k_l)y) \tag{23}$$

$$\dot{y} = v + d \tag{24}$$

where δk_l denotes the 20% uncertainty of the spring stiffness and f is a nonlinear function representing the dynamics of E. To this model we associate the following observer:

$$\dot{\Delta} = L_1 \text{sign}(z_1 - \Delta) \tag{25}$$

$$\dot{\hat{v}} = \frac{1}{m+m_0}(\Delta - bz_2 - k_l\hat{y}) + L_2\text{sign}(z_2 - \hat{v}) \tag{26}$$

$$\dot{\hat{y}} = \hat{v} + L_3\text{sign}(y - \hat{y}) \tag{27}$$

where L_1, L_2 and L_3 are the observer gain and z_1 and z_2 are observer outputs defined by:

$$z_1 = \Delta + (m + m_0)L_2\text{sign}(z_2 - \hat{v}) \tag{28}$$

$$z_2 = \hat{v} + L_3\text{sign}(y - \hat{y}) \tag{29}$$

The observer state Δ is intended to estimate the expression $E = S_1P_1 - S_2P_2$.

To prove the efficiency of the observer and that the estimated states based controller can also achieve accurate positioning in presence of perturbation and uncertainty, we will proceed by a step by step proof.

Step 1: Let $e_y = y - \hat{y}$ and $e_v = v - \hat{v}$, from (24) and (27) the error dynamics are expressed as:

$$\dot{e}_y = e_v + d - L_3\text{sign}(e_y) \tag{30}$$

Thus, if L_3 is chosen such that:

$$L_3 > \sup_{t>0}\{e_v(t) + d\} \tag{31}$$

then a sliding mode is established at the observer sliding surface $e_y = 0$ within a finite time. Moreover, at sliding mode we obtain $\dot{e}_y = 0$ and thus from (30) we have

$$0 = v - \hat{v} + d - L_3\text{sign}(e_y) \tag{32}$$

that is

$$v + d = \hat{v} + L_3\text{sign}(e_y) = z_2 \tag{33}$$

At this step, we may deduce that the observer state $\hat{y}$ will converge within a finite time to the system state y and meanwhile the observer output z_2 will converge to the perturbed rod velocity $v + d$.

Step 2: Let $e_\Delta = E - \Delta$ and taking into account that $e_y = 0$ and $z_2 = v + d$, then from (23) and (26) the error dynamics are expressed as follows:

$$\dot{e}_v = \frac{1}{m+m_0}\Big(e_\Delta + bd - \delta k_l y\Big) - L_2\text{sign}(e_v + d) \tag{34}$$

Thus, if L_2 is chosen such that:

$$L_2 > \sup_{t>0}\{e_\Delta(t) + bd_{\max} - \delta k_l y(t)\} \tag{35}$$

then we can deduce that $e_v + d$ tend to zero and hence $\hat{v}$ tend to $v + d$. That is the observer state $\hat{v}$ will reach its output z_2. Moreover, when the error dynamics are sliding on $e_y = 0$ and $e_v + d = 0$, then $\dot{e}_v = 0$ and we get:

$$E + bd - \delta k_l y = \Delta + (m + m_0)L_2\text{sign}(z_2 - \hat{v}) = z_1 \tag{36}$$

That is the observer will estimate the expression $E = S_1P_1 - S_2P_2$ with a constant difference proportional to the perturbation d and the uncertainty δk_l. Eventually, when the estimated variables are used to design the sliding surface, then the uncertainty will be taken into consideration, therefore when the controller sliding mode is reached the convergence to the reference position is obtained despite the existence of the constant perturbation d which will be annihilated by the use of the integral action in the surface definition.

Figure 12 shows the convergence of the observer state $\hat{y}$ to y although starting from different initial conditions; $y(0) = 0$ and $\hat{y}(0) = -0.1$ that is the observer starting at -10cm. As expected from the above analysis, $\hat{v}$ tends to $v + d$ and Δ tends to E with a constant difference. The observer gains are chosen as $L_1 = 10^7$, $L_2 = 3000$ and $L_3 = 30$. The system behavior is shown on Fig. 13 with the sliding surface being calculated using the estimated states and the controller with a smooth saturation function.

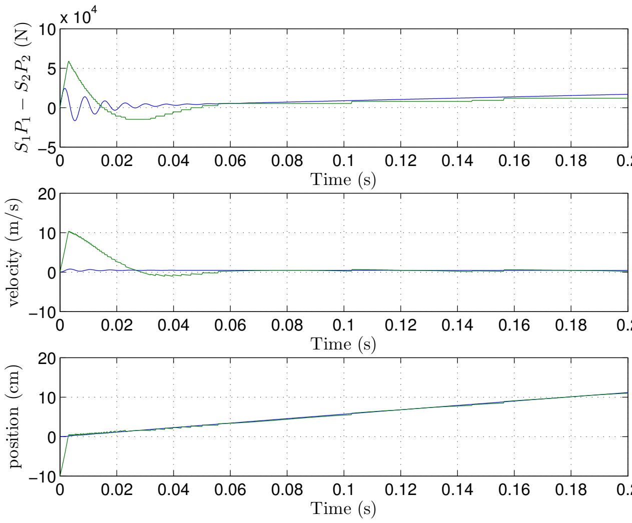

Fig. 12. Convergence of the sliding mode observer to the intended values.

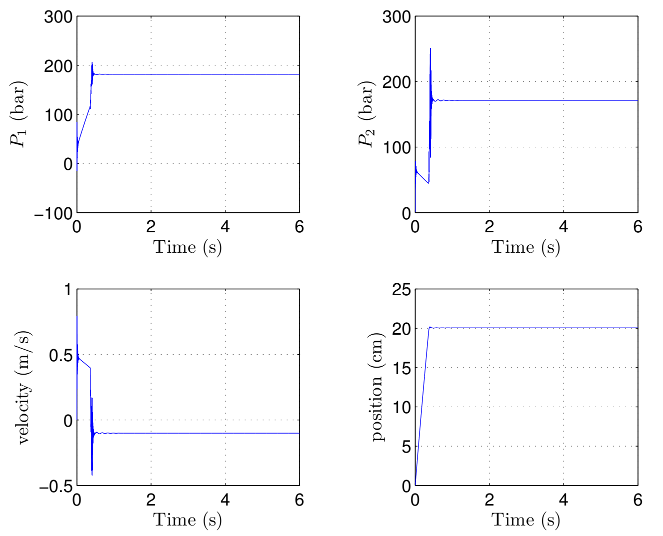

Fig. 13. Behavior of the hydraulic servo system controlled with sliding mode controller with estimated states feedback.

5. CONCLUSION

In this paper, a method to design an integral-sliding mode controller with a realizable reference was suggested in order to overcome the wind-up phenomenon due to the actuator saturation. The controller achieves zero steady state error with a substantially short settling time. The controller is compared to the PI controller and the plain sliding mode controller and has been shown to outperform them in terms of rapidity. To diminish the chattering effects, a smooth saturation function has been used to substitute the sharp discontinuous sign function. Finally, we have suggested the use of sliding observer to achieve an output feedback control and design the sliding surface using the observer estimations.

APPENDIX

Proof of *Proposition 1*:

By assumption of exponential stability of (11a) we have $\lim_{t\to\infty} x_1(t) = 0$ if $u(x_1, x_2)$ is bounded. Thus, we need to show that $\|x_2\| < \infty$.

The exponential boundedness of $\dot{x}_2 = f_2(x_{1e}, x_2 + x_{2e})$ implies that there exist $V(x_2)$ such that the following hold outside a ball of radius R for some positive constants a_1, a_2, a_3 and a_4 (Sastry and Isidori, 1989).

$$a_1\|x_2\|^2 \le V(x_2) \le a_2\|x_2\|^2 \ , \tag{37a}$$

$$\frac{dV}{dx_2} f_2(x_{1e}, x_2 + x_{2e}) \le -a_3\|x_2\|^2 \ , \tag{37b}$$

$$\left\|\frac{dV}{dx_2}\right\| < a_4\|x_2\| \ . \tag{37c}$$

Combining (11b) and (37b) yields

$$\begin{aligned}\dot{V} &= \frac{dV}{dx_2} f_2(x_1 + x_{1e}, x_2 + x_{2e}) \\ &\le -a_3\|x_2\|^2 \\ &\quad + \frac{dV}{dx_2}.\big(f_2(x_1 + x_{1e}, x_2 + x_{2e}) - f_2(x_{1e}, x_2 + x_{2e})\big) \ , \\ &\le -a_3\|x_2\|^2 + a_4\|x_2\|.\gamma_1\gamma_3 \ ,\end{aligned}$$

thus

$$\dot{V} \le 0 \quad \text{for} \quad \|x_2\| \ge \frac{a_4\gamma_1\gamma_3}{a_3} \ . \tag{38}$$

Using (37) and (38) it follows that any trajectory of $x_2(t)$ starting at a finite value $x_2(0)$ will eventually enter a ball of radius $\bar{R} = \max\{R, \frac{a_4\gamma_1\gamma_3}{a_3}\}$ therefore $\|x_2\| < \infty$ and $\lim_{t\to\infty} x_1(t) = 0$ is achieved. □

NOMENCLATURE

Parameter	value	unit
	fluid	
B	2.2×10^9	Pa
P_s	300×10^5	Pa
P_r	1×10^5	Pa
	piston	
m_0	50	kg
S_1	3.1×10^{-3}	m^2
S_2	1.5×10^{-3}	m^2
V_0	0.458×10^{-3}	m^3
	load	
m	20	kg
b	590	kg/s
k_l	125000	N/m
	servovalve	
k	1.46×10^{-5}	$m^3s^{-1}A^{-1}Pa^{-1/2}$
α	4.605×10^{-13}	$m^3s^{-1}Pa^{-1}$
γ	10622	s^{-1}
	Controller	
$u_{\max}$	20	mA
y_{ref}	0.2	m
k_0	0.5	–
k_i	0.5	–

REFERENCES

Ahn, K.K. and Dinh, Q.T. (2009). Self-tuning of quantitative feedback theory for force control of an electro-hydraulic test machine. *Control Engineering Practice*, 17(11), 1291 – 1306.

Aly, A.A. (2011). Pid parameters optimization using genetic algorithm technique for electrohydraulic servo control system. *Intelligent Control and Automation*, 2, 69 – 76.

Bonchis, A., Corke, P., Rye, D., and HA, Q. (2001). Variable structure methods in hydraulic servo systems control. *Automatica*, 37, 589–595.

Chen, H.M., Renn, J.C., and Su, J.P. (2005). Sliding mode control with varying boundary layers for an electro-hydraulic position servo system. *The International Journal of Advanced Manufacturing Technology*, 26(1-2), 117–123.

Feki, M., Richard, E., and Gomes Almeida, F. (1999). Commande en effort d'un vérin hydraulique par linéarization entrée/sortie. In *Journées Doctorales d'Automatiques, JDA'99.*, 181–184. Nancy-France.

Feki, M. and Richard, E. (2005). Including leakage flow in the servovalve static model. *Int. J. of Modelling and simulation*, 25(1), 4004–4009.

Guan, C. and Pan, S. (2008). Nonlinear adaptive robust control of single-rod electro-hydraulic actuator with unknown nonlinear parameters. *Control Systems Technology, IEEE Transactions on*, 16(3), 434–445.

Has, Z., Rahmat, M.F., Husain, A.R., Ishaque, K., Ghazali, R., Ahmad, M.N., Sam, Y.M., and Rozali, S.M. (2013). Robust position tracking control of an electro-hydraulic actuator in the presence of friction and internal leakage. *Arabian Journal for Science and Engineering*, 1–14.

Hwang, C. and Lan, C. (1994). The position control of electrohydraulic servomechanism via a novel variable structure control. *Mechatronics*, 4(4), 369 – 391.

Indrawanto, T.B. (2011). Sliding mode control of a single rigid hydraulically actuated manipulator. *International Journal of Mechanical & Mechatronics Engineering*, 11, 1–9.

Jian-jun, Y., Duo-tao, D., Gui-lin, J., and Sheng, L. (2012). High precision position control of electro-hydraulic servo system based on feed-forward compensation. *Research Journal of Applied Sciences, Engineering and Technology*, 4(4), 289 – 298.

Khebbache, H. and Tadjine, M. (2013). Robust fuzzy backstepping sliding mode controller for a quadrotor unmanned aerial vehicle. *Journal of Control Engineering and Applied Informatics*, 15(2), 3 – 11.

Kolsi-Gdoura, E., Feki, M., and Derbel, N. (2013). Sliding mode-based robust position control of an electrohydraulic system. In *Int. Multi-Conference on Systems, Signals and Devices (SSD'13)*, 1–6. IEEE, Hammamet-Tunisia.

Merritt, H.E. (1967). *Hydraulic Control Systems*. John Wiley & Sons, USA.

Miao, Z., liang Liu, C., yong Wang, X., and Zha, X.F. (2008). High precision control for hydraulic servo systems with large frictional torques and experimental research. *European Journal of Control*, 14(5), 437 – 444.

Mihajlov, M., Nikolić, V., and Antić, D. (2002). Position control of an electro-hydraulic servo system using sliding mode control enhanced by fuzzy pi controller. *Mechanical Engineering*, 1(9), 1217 – 1230.

Rossomando, F.G., Soria, C., and Carelli, R. (2014). Sliding mode control for trajectory tracking of a non-holonomic mobile robot using adaptive neural networks. *Journal of Control Engineering and Applied Informatics*, 16(1), 12 – 21.

Sastry, S.S. and Isidori, A. (1989). Adaptive control of linearizable systems. *IEEE Trans. on Automatic Control*, 34(11), 1123–1131.

Sirouspour, M. and Salcudean, S. (2000). On the nonlinear control of hydraulic servo-systems. In *IEEE International Conference on Robotics and Automation, 2000.*, volume 2, 1276–1282.

Tafazoli, S., De Silva, C.W., and Lawrence, P.D. (1998). Tracking control of an electrohydraulic manipulator in the presence of friction. *IEEE Trans. on Control Systems Technology*, 6(3), 401–411.

Truong, D.Q. and Ahn, K.K. (2009). Force control for hydraulic load simulator using self-tuning grey predictor – fuzzy pid. *Mechatronics*, 19(2), 233 – 246.

Ursu, I., Toader, A., Halanay, A., and Balea, S. (2013). New stabilization and tracking control laws for electrohydraulic servomechanisms. *European Journal of Control*, 19(1), 65 – 80.

Viersma, T.J. (1980). *Analysis, Synthesis, and Design of Hydraulic Servosystems and Pipelines.* Elsevier, Netherlands.

Yao, B., Bu, F., and Chiu, G.T.C. (2001). Non-linear adaptive robust control of electro-hydraulic systems driven by double-rod actuators. *International Journal of Control*, 74(8), 761–775.